

## Class of Molecular and Solid State Systems with Correlated Magnetic and Dielectric Bistabilities Induced by the Pseudo Jahn-Teller Effect

Pablo Garcia-Fernandez<sup>1</sup> and Isaac B. Bersuker<sup>2</sup>

<sup>1</sup>*Ciencias de la Tierra y Física de la Materia Condensada, Universidad de Cantabria, Avenida de los Castros s/n, E-39005, Santander, Spain*

<sup>2</sup>*Institute for Theoretical Chemistry, The University of Texas at Austin, Chemistry and Biochemistry Department, Austin, Texas 78712-0164, USA*

(Received 14 April 2011; published 17 June 2011)

Based on the earlier revealed hidden pseudo Jahn-Teller effect which essentially involves excited electronic states we show that, with extension to solids, polyatomic systems with half-filled degenerate shells,  $e^2$  or  $t^3$ , form a novel (practically inexhaustible) class of molecular and solid state materials with correlated and switchable magnetic and dielectric bistabilities. The latter are confirmed by state-of-the-art *ab initio* calculations, including estimation of lifetimes, for several representatives of this class, which also reveal a giant magnetoelastic effect in  $\text{LiCuO}_2$  and  $\text{NaCuO}_2$  crystals.

DOI: [10.1103/PhysRevLett.106.246406](https://doi.org/10.1103/PhysRevLett.106.246406)

PACS numbers: 71.70.Ej, 33.15.Kr, 75.30.Wx, 75.80.+q

Molecular systems and solids with two coexisting stable and close-in-energy configurations that exhibit markedly different magnetic and structural properties with controllable conversion between them (bistability) are very attractive for application in electronics as high-density information storage materials and sensor devices [1–5]. With regard to molecular magnetic bistability the most studied systems so far, apart from the single-molecule magnets [6], involve some specific transition metal spin crossover (TMSC) complexes for which the low-spin (LS) to high-spin (HS) transition can be induced by temperature or pressure changes or by light irradiation [4,5]. However, in spite of almost three decades of study of such systems, the room-temperature lifetime of their metastable state in isolated complexes is typically a few nanoseconds [4,5], which is too short for practical application. Cooperative effects [7,8] between a few thousands of these complexes may extend their lifetime at the cost of substantially increasing the size of the material.

On the other hand, it was shown recently [9] that in molecular systems with at least one threefold (or higher) symmetry axis and a half-filled degenerate valence shell (valence orbital configurations  $e^2$  or  $t^3$ , where  $e$  and  $t$  are symmetrized molecular orbitals), a similar to the spin-crossover (but richer) bistability effect takes place. These configurations have totally symmetric charge distribution and no Jahn-Teller effect (JTE), but they possess hidden pseudo JTE (PJTE [10]). According to Hund's rule the two (in  $e^2$ ) or three (in  $t^3$ ) electrons should have parallel spins in the ground state, but the PJTE mixing between two low-lying low-spin excited states produces an additional low-spin state accompanied by structural distortions [9], as illustrated in Fig. 1. The PJT mechanism explains why and how orbital disproportionation and additional covalency lead to the formation of the second stable state [9]. The two equilibrium configurations in such molecular systems

are close in energy and have different spin values (magnetic bistability) and geometries (structural bistability). Both bistabilities are strongly correlated and are switchable by external perturbations.

In this Letter the idea that the PJTE in two excited states produces an additional equilibrium configuration with a different spin [9] is extended to solid states and confirmed by *ab initio* simulations including calculations of temperature dependent lifetimes, thus showing that the vast variety of systems with a common special feature of electronic structure—half-filled degenerate valence shells—form a class of bistability systems which can be termed half-filled-shell (HFS) systems. We show also that both in molecular systems and solids the PJTE induced bistabilities have not only much better parameters and lifetimes (by orders of magnitude) than the TMSC magnetic bistability, but are accompanied by symmetry breaking that changes from nonpolar to dipolar or quadrupolar structures (dielectric bistability) (Fig. 1). In addition, some of these systems in the solid state may display also strong magnetoelastic and ferroelastic properties, and all these effects can be tuned by means of external perturbations. As the number of molecular and solid state systems with  $e^2$  and  $t^3$  electronic configurations is practically infinite and they may occur in all aggregate states of matter formed by organic and inorganic, main group, and transition metal compounds in all varieties of crystal structures and impurity centers in crystals, as well as in solutions, clusters, quantum dots, and thin films, we thereby suggest an inexhaustible source of systems with potential bistability properties.

The common properties of HFS systems and their origin can be illustrated using the  $\text{CuF}_3$  molecule as an example. In the high-symmetry configuration this molecule is planar regular-triangular with  $D_{3h}$  symmetry and the electron configuration  $e^2$ . Figure 2 shows the results of *ab initio* calculations of its ground and excited electronic states as a

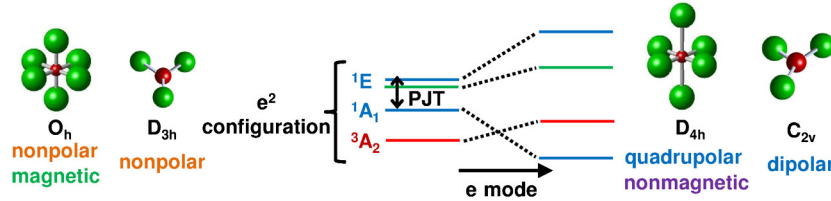


FIG. 1 (color online). The  $e^2$  electronic configuration spans the states  ${}^3A_2$ ,  ${}^1A_1$ , and  ${}^1E$ . While the magnetic  ${}^3A_2$  state is lowest in energy and stable for the high-symmetry configuration (left) the excited states interact through the PJT effect leading to a low-energy distorted equilibrium configuration with different properties (right).

function of the angle  $\alpha$ (FCuF). We see that when the molecule is an equilateral triangle ( $\alpha = 120^\circ$ ) the ground state is  ${}^3A'_2$  with the lowest excited states  ${}^1A'_1$  and  ${}^1E'$ , which is typical for all electronic  $e^2$  configurations (Fig. 1). The spin-triplet ground state  ${}^3A'_2$  in this  $D_{3h}$  geometry is stable, but there is a strong PJT coupling between the two excited states  ${}^1A'_1$  and  ${}^1E'$  by  $e'$ -type distortions due to which the lower state  ${}^1A'_1$  goes down, crosses the  ${}^3A'_2$  state, and produces a global minimum in which the initial geometry  $D_{3h}$  is reduced to  $C_{2v}$  and the electronic state is a spin-singlet  ${}^1A'_1$  (Figs. 1 and 2). As a result the molecule  $\text{CuF}_3$  has two stable states: the triplet (high-spin, HS) state has a magnetic moment of  $\mu_1 = 1.82$  MB and a zero dipole moment  $p_1 = 0$ , whereas the low-spin (LS) state has a zero magnetic moment  $\mu_2 = 0$  and a strong dipole moment of  $p_2 = 1.67$  D. The HS state is higher in energy by  $\Delta E \approx 0.2$  eV and it has an energy barrier of  $B \approx 0.33$  eV to the point of spin crossover with the LS state (energy values are read off the zero vibrations).

We have thus two coexisting bistabilities, magnetic and dielectric (dipolar), which are strongly correlated: you may have either a HS state with a zero dipole moment, or a zero spin state with nonzero dipole moment. Such correlations between magnetic and polar properties are typical for solid state multiferroics. Hence the  $\text{CuF}_3$  molecule may be termed as a single-molecule multiferroic. An ensemble of such molecules, e.g., organized as a thin film is a representative of HFS materials. With qualitatively the

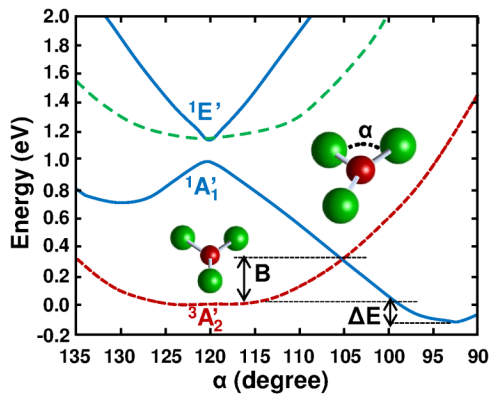


FIG. 2 (color online). *Ab initio* calculated energy levels of  $\text{CuF}_3$  as a function of the angle  $\alpha$  ( $e$  mode distortion) showing the formation of the two equilibrium configurations typical for HFS systems.

same picture of bistability different HFS systems have varying parameter values; some of them calculated *ab initio* are shown in Table I. Quite recently [11] this bistability effect has been observed directly in isolated molecules in solution containing a  $\text{Ni}^{2+}$  ion in the square-planar environment of the Ni-tetrakis (pentafluorophenyl) porphyrin complex which has the features of the electronic  $e^2$  configuration (energy terms of Fig. 1), and is thus a HFS system representative. This molecule displays two magnetic states with a low spin ( $S = 0$ ) in the square-planar configuration and high spin ( $S = 1$ ) in the distorted pentacoordinated geometry, respectively, in accordance with the general conclusions outlined in Ref. [9] and in this Letter. The two states are switchable by optical irradiation, and they have 27-hour half-lifetimes at room temperature. This observed bistability is a perfect example confirming our conclusions in this Letter and in Ref. [9]; the authors [11] do not discuss its origin.

The idea of PJTE bistabilities can be extended to solid state systems in which case the HFS,  $e^2$  or  $t^3$ , are formed by either localized orbitals on the centers or corresponding band states. Solid state HFS systems may be more important in applications because of their larger variety and better parameters. They may include virtually all the trigonal and cubic symmetry coordination compounds, ionic crystals, and impurity centers in crystals containing transition metal ions with the electronic configuration  $e^2$  ( $d^8$  ions in octahedral coordination and  $d^2$  ions in trigonal, tetrahedral, or cubic environment), and  $t^3$  ( $d^3$  in octahedral and  $d^7$  in tetrahedral coordination). Remarkably, that for these  $d^n$  electronic configurations TMSC is not possible. Similar to the mentioned above observed bistability in a

TABLE I. HS-LS distortions, symmetry-breaking  $Q_{sb}$  and totally symmetric  $Q_{ts}$  (in Å), energy difference  $\Delta E$ , barrier  $B$  (read off the zero-point energy) (in eV), and lifetimes  $\tau$  (in s) at low temperatures ( $T = 5$  K) calculated by two methods for several HFS systems.

System	$Q_{sb}$	$Q_{ts}$	$\Delta E$	$B$	$\beta$	$\tau_1$	$\tau_2$
$\text{Si}_3$	0.34	0.06	0.17	0.12	340	$1.2 \times 10^{-7}$	$1.4 \times 10^{-7}$
$\text{CuF}_3$	0.61	0.20	0.21	0.33	1040	$2.9 \times 10^{-5}$	$9.1 \times 10^{-5}$
$\text{Si}_4$	0.82	0.22	1.08	0.72	166	$3.0 \times 10^0$	$8.4 \times 10^{-2}$
$\text{Ge}_4$	0.79	0.05	0.82	0.81	1940	$2.6 \times 10^4$	$3.5 \times 10^0$
$\text{C}_4\text{H}_4$	0.56	0.06	0.78	0.13	1.2	$3.7 \times 10^{-6}$	$4.4 \times 10^{-6}$
$\text{CuO}_6$	1.24	0.46	0.23	0.17	890	$6.7 \times 10^{14}$	$1.4 \times 10^{17}$

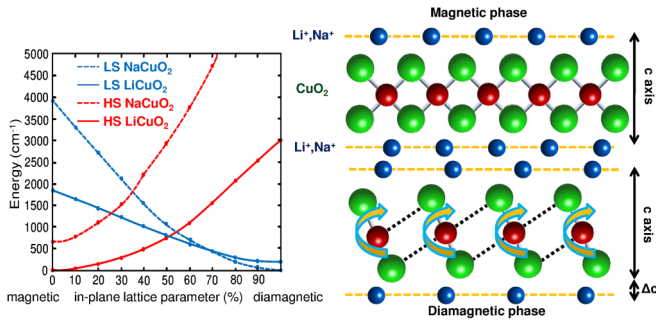


FIG. 3 (color online). Calculated relative stability of the  $\text{LiCuO}_2$  and  $\text{NaCuO}_2$  crystals in the magnetic to diamagnetic transition as a function of the in-plane lattice parameter: at  $\sim 35\%$  of strain in  $\text{NaCuO}_2$  and  $\approx 50\%$  in  $\text{LiCuO}_2$  the two phases become approximately degenerate. The distortion along the  $c$  axis is also illustrated.

$\text{Ni}^{2+}$  ( $d^8$ ) complex in solution [11], there is experimental evidence of a reversible equilibrium between octahedral magnetic and square-planar diamagnetic complexes of this ion in solid states [12,13].

We performed electronic structure calculations for two solids from the HFS class, the crystals  $\text{LiCuO}_2$  and  $\text{NaCuO}_2$ . Their lattices contain alternating layers of vertex-sharing  $\text{Cu}^{3+}(\text{O}^{2-})_6$  octahedrons and  $\text{Li}^+$  or  $\text{Na}^+$  ions, respectively (Fig. 3). The  $\text{Cu}^{3+}$  ion has a  $(d^8)e^2$  electronic configuration (as above,  $e$  denotes either molecular orbitals or symmetrized band states). The results of density functional theory (DFT) calculations employing the hybrid B1WC functional [14] with geometry optimization of the two crystal structures in both the HS (ferromagnetic and antiferromagnetic) and LS (diamagnetic) states are shown in Fig. 3 and the supplemental material [19]. As predicted by the general theory and shown above for molecular cases, the HS configuration of these crystals is undistorted, while the LS state is diamagnetic with a very strong elongation of the  $\text{CuO}_6$  octahedrons (Figs. 1 and 3). The ferromagnetic and antiferromagnetic phases have very similar local geometries with regular octahedral coordination of the oxygen atoms around Cu, whereas the diamagnetic phase is strongly distorted to almost square-planar coordination: in  $\text{LiCuO}_2$  the metal-ligand distance in the magnetic phase is 2.01 Å, while in the diamagnetic phase the equatorial and axial ligands are at 1.86 Å and 2.76 Å, respectively. In  $\text{NaCuO}_2$  the same pattern is found, although the lattice parameter and distortions are by about 10% larger than in  $\text{LiCuO}_2$ . The results obtained for the geometry of the diamagnetic phase of these crystals agree well (within 2%) with the experimental data [15,16]; the interatomic distance differences in the two phases are here 3–4 times larger than in the two spin states of TMSC systems.

The magnetic to diamagnetic phase transition has a strong repercussion on the crystal structure along the  $c$  axis enlarging the unit cell by 10% (0.5 Å), but the geometrical difference between the two bistability states

does not translate in a large energy difference between them. Indeed, in Fig. 3 the energy difference between the phases is only of a few hundred  $\text{cm}^{-1}$ . In the case of  $\text{LiCuO}_2$  the calculations yield that the magnetic phase (at the minimum of the APES) is lower by 150  $\text{cm}^{-1}$  than the diamagnetic one, but with the vibrational zero-point-energy correction the two phases are almost degenerate. In  $\text{NaCuO}_2$  the nonmagnetic phase is more stable. Because of the small energy differences between the phases it should be relatively easy to trigger a phase transition between them by external perturbation. Indeed, for  $\text{LiCuO}_2$  a phase transition [17] is observed at  $T = 180$  K. For  $\text{NaCuO}_2$  our *ab initio* calculations show that a diamagnetic to magnetic phase transition is achievable at a pressure of  $\approx 6$  GPa.

In view of the close energy values of the two phases we explored the possibility to further tune the system by means of epitaxial strain, so that they become almost degenerate and hence more vulnerable to external perturbations. The in-plane geometry of the unit cell of these crystals is almost hexagonal, so their growth on a particular hexagonal substrate could constrain the in-plane lattice constant. We have performed geometry optimizations with the in-plane lattice parameters fixed to a value between those of the magnetic phase and the diamagnetic phase while the rest of the parameters were let free to vary. The results show that at some intermediate strains ( $\approx 50\%$  for  $\text{LiCuO}_2$ ,  $\approx 35\%$  for  $\text{NaCuO}_2$ , see Fig. 3) where the magnetic and nonmagnetic phases become degenerate (and hence a diamagnetic to magnetic phase transition can be triggered by a magnetic field) there is a strong distortion of the crystal along the  $c$  axis; the lattice parameter of  $\text{LiCuO}_2$  ( $\sim 5$  Å) changes by  $\approx 0.2\%$  which amounts to  $\sim 1$  pm. Such changes in lattice parameters are typical in ferroelectrics, but very seldom found in magnetic transitions. In fact such distortions are termed as giant magnetoelastic effects (see, e.g., [18]). Moreover, a similar change in the lattice parameter of  $\text{NaCuO}_2$  is  $\approx 0.8\%$ , almost 4 times larger than those of  $\text{LiCuO}_2$ . In the strained systems this change in lattice parameter is realized by a tilting of the  $\text{CuO}_2$  (almost) square-planar units in the diamagnetic phase toward the formation of  $\text{CuO}_6$  octahedrons by the near neighbor rows in the magnetic phase (Fig. 3).

One of the most important characteristics of the bistability with regard to possible applications is the lifetime  $\tau$  (relaxation time) of the induced higher in energy state (in cases in Table I the spin-triplet state) with respect to its thermal relaxation to the lower (spin-singlet) state. This is less a problem for solids where the cooperative interactions stabilize well the two states in the bistability. For molecular systems or small aggregates the relaxation lifetime depends on several factors, mainly on the spin-orbital interaction, the barrier height and width between the two minima of the APES, and the dissipation of energy in interaction with the environment. Direct calculation of  $\tau$  is not trivial; we employed two approaches to get more



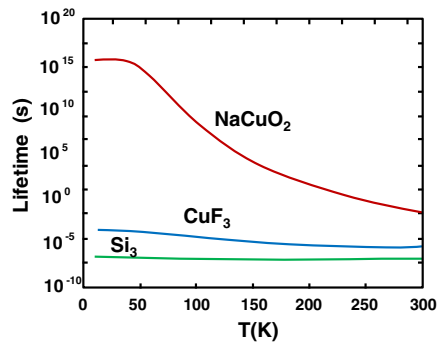


FIG. 4 (color online). Temperature dependence of lifetimes estimated for the higher in energy high-spin states of  $\text{Si}_3$ ,  $\text{CuF}_3$  and an isolated octahedral center in  $\text{NaCuO}_2$  by means of model calculations following Ref. [4].

reliable results. In the first one we start from the time-dependent Schrödinger equation and follow the evolution of the system in the presence of a dissipation factor  $\gamma$  that describes the thermalization time of the vibrational levels of the system in the singlet state. The second method, developed for TMSC [4,5] is simpler, but it is applicable when there is only one-mode distortion in the transition between the two configurations. More details on lifetime calculations are given in the supplemental material [19].

Table I shows the results of calculation of the HS configuration lifetime for several molecular systems and for (isolated) octahedral units in  $\text{LiCuO}_2$  carried out by the two methods, while Fig. 4 illustrates the temperature dependence of some of them. As expected, the distortions in all HFS systems are dominated by the symmetry-breaking coordinate ( $Q_{\text{sb}}$ ) (in normal TMSC systems they are dominated by  $Q_{\text{ts}}$ ) and in general they are larger or much larger than in the TMSC systems. The structural changes increase essentially the lifetime of HFS systems as compared with TMSC because of the strong dependence of the coupling constant on the overlap of the vibrational functions of the two states (see supporting information). Along this line the system with larger lifetime is the  $\text{CuO}_6$  complex in  $\text{LiCuO}_2$  due to its large distortion ( $Q_{\text{sb}} = 1.24 \text{ \AA}$ ) followed by  $\text{Ge}_4$  and  $\text{Si}_4$  clusters ( $Q_{\text{sb}} \approx 0.8 \text{ \AA}$ ). An increase in  $\tau$  is also achieved in organic and other compounds of nonheavy elements due to their smaller spin-orbital coupling constant.

In Table I  $\text{Si}_3$  has the shortest lifetime which increases in systems with larger distortions and reaches macroscopic values in  $\text{Si}_4$ ,  $\text{Ge}_4$ , and  $\text{LiCuO}_2$  at low temperatures (but in  $\text{Ge}_4$  there are low-lying triplet excited states that may reduce the lifetime). In the crystals  $\text{LiCuO}_2$  and  $\text{NaCuO}_2$  the estimates of the lifetime of the HS configuration are carried out for a separate cluster unit  $\text{CuO}_6$ ; it is extremely large at low temperatures (due to the large distortions in the diamagnetic phase) and remains macroscopic at room temperature. Since the cooperative interactions between the complexes in the condensed phases obviously increase the lifetimes, the values in Table I and in Fig. 4 show the

lower limit of the expected lifetimes. This means that the crystals  $\text{LiCuO}_2$  and  $\text{NaCuO}_2$  are quite feasible for practical use as bistability materials, and their large lifetime of both states in this bistability indicates that they can be used in the form of clusters, quantum dots, or thin films.

In conclusion, we revealed a whole class of molecular and solid state systems with a common feature of electronic structure,  $e^2$  or  $t^3$ , that have the potential of serving as materials with bistability properties important to a variety of applications. A recent experimental work observed it directly in a HFS system in solution that has the two switchable magnetic and structural states and a 27-hour half-lifetime of the less stable configuration at room temperatures. For two crystals,  $\text{LiCuO}_2$  and  $\text{NaCuO}_2$ , the bistability properties are shown to be tunable, and they may possess a giant magnetoelastic effect.

This work was supported by Welch Foundation Grant No. F-100 and the Spanish Ministerio de Ciencia y Tecnologia under Project No. FIS2009-07083.

- [1] O. Kahn and C.J. Martinez, *Science* **279**, 44 (1998).
- [2] J.-P.E. Sauvage, *Struct. Bond.* **99**, 1 (2001).
- [3] B.L. Feringa, R.A. van Delden, N. Koumura, and E.M. Geertsema, *Chem. Rev.* **100**, 1789 (2000).
- [4] A. Hauser, C. Enachescu, M.L. Daku, A. Vargas, and N. Amstutz, *Coord. Chem. Rev.* **250**, 1642 (2006).
- [5] F. Renz, H. Oshio, V. Ksenofontov, M. Waldeck, H. Spiering, and P. Gütllich, *Angew. Chem., Int. Ed.* **39**, 3699 (2000).
- [6] D. Gatteschi, R. Sessoli, and J. Villain, *Molecular Nanomagnets* (Oxford University Press, New York, 2006).
- [7] J. Larionova, L. Salmon, Y. Guari, A. Tokarev, K. Molvinger, G. Molnar, and A. Bousseksouet, *Angew. Chem., Int. Ed.* **47**, 8236 (2008).
- [8] I. Boldog, A.B. Gaspar, V. Martinez, V. Pardo-Ibañez, V. Ksenofontov, A. Bhattacharjee, P. Gütllich, and J.A. Real, *Angew. Chem., Int. Ed.* **120**, 6533 (2008).
- [9] P. Garcia-Fernandez, I.B. Bersuker, and J.E. Boggs, *J. Chem. Phys.* **125**, 104102 (2006).
- [10] I.B. Bersuker, *The Jahn-Teller Effect* (Cambridge University Press, Cambridge, U.K., 2006).
- [11] S. Venkataramani *et al.*, *Science* **331**, 445 (2011).
- [12] Y. Ihara and T. Ryokichi, *Bull. Chem. Soc. Jpn.* **57**, 2829 (1984).
- [13] M.M. Hoffmann, J.G. Darab, B.J. Palmer, and J.L. Fulton, *J. Phys. Chem. A* **103**, 8471 (1999).
- [14] D.I. Bilc, R. Orlando, R. Shaltaf, G.-M. Rignanese, J. Iniguez, and P. Ghosez, *Phys. Rev. B* **77**, 165107 (2008).
- [15] R. Berger and L.-E. Tergenius, *J. Alloys Compd.* **203**, 203 (1994).
- [16] J. Pickardt, W. Paulus, M. Schmalz, and C. Schollhorn, *J. Solid State Chem.* **89**, 308 (1990).
- [17] F.J. Owens, *Physica (Amsterdam)* **313C**, 65 (1999).
- [18] S. Lee *et al.*, *Nature (London)* **451**, 805 (2008).
- [19] See supplemental material at <http://link.aps.org/supplemental/10.1103/PhysRevLett.106.246406> for computational details and the structural information on  $\text{NaCuO}_2$  and  $\text{LiCuO}_2$ .